Views

Samuel Arba-Mosquera*, Luise Krüger, Pascal Naubereit, Simas Sobutas, Shwetabh Verma, Len Zheleznyak and Wayne H. Knox

Analytical optimization of the laser induced refractive index change (LIRIC) process: maximizing LIRIC without reaching the damage threshold

https://doi.org/10.1515/aot-2021-0052
Received October 22, 2021; accepted October 29, 2021;
published online November 19, 2021

Abstract: A method to determine the optimum laser parameters for maximizing laser induced refractive index change (LIRIC) while avoiding exceeding the damage threshold for different materials with high water content (in particular, polymers such as hydrogels or the human cornea) is proposed. The model is based upon two previous independent models for LIRIC and for laser induced optical breakdown (LIOB) threshold combined in a simple manner. This work provides qualitative and quantitative estimates for the parameters leading to a maximum LIRIC effect below the threshold of LIOB.

Keywords: femtosecond lasers; laser induced optical breakdown; laser induced refractive index change.

1 Introduction

Since the introduction by Trokel [1] of the excimer laser surgery of the cornea in 1983, more than 70 million treatments have been successfully performed. As the prevalence of myopic defects in western societies is about 30% and of above 50% in Asian countries [2], the potential of the surgical techniques reaches more than 1 billion people (without consideration of their economic means).

A number of authors have considered the problems observed in refractive surgery, developing experimental animal models for analyzing PRK [3], LASIK [4], LASEK, CXL [5], corneal additive surgery [6], as well as the investigations of the corneal cauterization [7] and induction of corneal haze [8, 9].

With recent advances to laser technologies [10, 11] for refractive surgery [12], the change of the corneal curvature to compensate in a controlled manner for refractive errors of the eye [13] is more accurate than ever. The procedure is now a successful technique, due to its submicron precision and the high predictability and repeatability of corneal ablation [14] while minimizing side-effects [15]. Standard ablation profiles based on the removal of convex–concave tissue lenticules with spherocylindrical surfaces proved to be effective in the compensation of primary refractive errors [16], however the quality of vision deteriorated significantly, especially under mesopic and low-contrast conditions [17]. Furthermore, there is still debate concerning the optimal technique for corneal refractive procedures [18], and about in which corneal layer to perform refractive procedures to maximize patients' visual outcomes.

The introduction of femtosecond lasers in ophthalmology has provided a platform for the development of many new refractive procedures and techniques in the last decades. These techniques have been shown to provide more reliability and cater to a wider spectrum of cases.

Femtosecond assisted LASIK [19] (FemtoLASIK): The goal of this procedure is to correct any ametropia that may be present in the eye, with the aim of retaining the epithelium as undamaged as possible. For this procedure, a flap is created and the stroma is exposed; the laser ablation is applied directly on the stroma. After the procedure, the flap is repositioned and allowed to heal naturally.

***Corresponding author: Samuel Arba-Mosquera**, SCHWIND Eye-Tech-Solutions, Kleinostheim, Germany, E-mail: sarbamo@cofis.es.
https://orcid.org/0000-0002-3152-0557
Luise Krüger, Pascal Naubereit and Shwetabh Verma, SCHWIND eye-tech-solutions, Kleinostheim, Germany
Simas Sobutas, Light Conversion, Vilnius, Lithuania
Len Zheleznyak, Clerio Vision, Inc., Rochester, NY, USA
Wayne H. Knox, Clerio Vision, Inc., Rochester, NY, USA; The Institute of Optics, University of Rochester, Rochester, USA; and Center for Visual Science, University of Rochester, Rochester, USA

The only difference between FemtoLASIK and regular LASIK is the technique for making the corneal flap. Instead of applying mechanical ways, the corneal flap is made with a femtosecond laser. This feature renders FemtoLASIK procedures their industry jargon of "Bladeless technology". Sub Bowman Keratomileusis [20] (SBK) is essentially similar to LASIK, only featuring a thinner flap created right under the Bowman's layer.

Femtosecond lenticule extraction [21] (FLEX): This procedure consists of creating a corneal flap and a lenticule with a femtosecond laser. This removed lenticule results in refractive correction; the corneal flap is then placed back and allowed to heal naturally. Small incision lenticule extraction [22] (SMILE): This procedure is essentially similar to FLEX, but no corneal flap is created in SMILE. The lenticule is removed via a small incision created at the edge of the treatment zone on the cornea.

In 1998 the use of the Nd:YLF picosecond laser as a nonmechanical microkeratome was first demonstrated, and the potential improvements of reducing laser pulse duration to the femtosecond regime were discussed [19]. Results were confirmed and applications expanded (Femto-LASIK, intracorneal ring segments, femtosecond laser keratomileusis, and intrastromal ablation) [23]. Creating corneal cuts like flaps for LASIK, lamellae for keratoplasty, pockets for corneal rings, and lenses or tunnels for corneal rings by using a laser device became more and more popular over the following years. The types of laser devices used in these applications came to be identified as "Femtosecond" (fs) lasers, for the characteristic pulse duration of the laser source. Particularly the quest for intrastromal lenticules was pursued since the inception of femtosecond lasers [24]. The first company to develop a commercial instrument realizing corneal flaps was Intralase, with which more predictable flap thickness [25, 26] and dimensions [27], better astigmatic neutrality [28], and decreased epithelial injury was demonstrated compared to two popular mechanical microkeratomes [29]. However, some specific femtoLASIK complications have been also discovered [30–33]. In general, it has been observed that by increasing the repetition rate of the femtosecond lasers, reducing pulse energies and using tighter spot spacing produces smoother flap surfaces [34]. Finally, the different optical and scanning configurations of the different femtosecond lasers systems seem to affect also the characteristics of the flap and of the procedure in general [35, 36].

The wavelength and the pulse duration are important parameters for both suprathreshold plasma formation creating cavitation bubbles [37] and safety. The plateau-like region observed between 100 fs and 1 ps for the corneal layers indicate that for use in laser surgery, laser pulse durations chosen within this range should give practically equivalent results.

Diode pumped all-solid-state ultrafast lasers are now widely used to perform minimally invasive refractive surgery and keratoplasty procedures. From its first clinical use in 2001 for LASIK flap creation, femtosecond lasers have steadily made a place as the dominant flap-making technology worldwide. Newer applications are being evaluated and are increasing in their frequency of use. Femtosecond laser technology is rapidly becoming a heavily utilized tool in corneal refractive surgical procedures due to its reproducibility, safety, precision, and versatility [38].

Small incision lenticule extraction (SMILE) is a relatively young technique, in use for more than 10 years [39]. It seems a very elegant technique to perform laser vision correction (LVC) involving only a femtosecond laser system [40]. While the origin of this technique dates back to 1995 (with the first patents filed by Escalon Medical) [41], nowadays in 2021 there are three platforms commercially available to perform these kind of treatments [42–44].

Several advantages have been put forward in favor of SMILE treatments, including corneal sensation, dry eye, and treatment duration [45]. But among all of them, probably the most interesting one would be the potential preservation of corneal biomechanical integrity to a larger extent than conventional LVC [46].

The major concern in LVC so far is the risk associated with cutting and removing tissue from the eye, necessarily severing to some extent corneal nerves, and weakening the cornea by removing stromal tissue, thus making the corneas thinner. Femtosecond lasers help reducing the impact of some of these aspects, and so does the SMILE technique. But a technique in which both these elements would be eliminated would be advantageous.

Nowadays, PiXL [47] is the only available surgical technique to perform refractive surgery without removing tissue or performing corneal cuts. But PiXL is also based on morphological modification of the corneal curvature and has its own issues mainly due to the use of UV-A radiation.

In contrast, LIRIC is a noncommercially available novel technique, allowing for the optical correction of refractive defects using a femtosecond laser system, yet *without the need to remove tissue or producing corneal cuts* [48]. Similarly, this technique is not based on the morphological modification of the corneal curvature, but on the inscribing of a lens into the cornea, by means of a so-called LIRIC which enables the local modification of the refractive index

of the corneal stroma to produce optical phase-shifts, which spatially combined, result in an optical correction. This technique has been developed in the last 14 years [49].

One of the concerns of LIRIC remains as to whether clinically meaningful phase-changes (a requirement for clinical optical correction) can be consistently achieved below the damage threshold of the materials, e.g., without inducing laser induced optical breakdown (LIOB) thus, without creating cavitation bubbles in the tissue. The aim of the current work is to present a simple theoretical framework (in the form of a combined model) to determine the optimum laser parameters for maximizing the LIRIC efficiency below the LIOB threshold.

2 Methods

2.1 LIRIC model

To describe the LIRIC process and quantify the induced phase-changes we based on the works by the group of Knox [50, 51]. The induced phase change after adequate laser irradiation can be given by

$$\Delta\phi = \gamma \frac{{P_{avg}}^{m} \cdot NA^{2(m-2)} \cdot m^{m-2}}{\upsilon^{m-1} \cdot \tau^{m-1} \cdot {\lambda_{write}}^{2m-3} \cdot \lambda_{read} \cdot S \cdot t}$$

where $\Delta\phi$ is the induced phase change for a given observer wavelength, γ is a material constant, P_{avg} the average power applied to the sample NA the numerical aperture of the optical system, m the order of the multiphoton absorption, ν the repetition rate of the laser irradiation, τ the pulse duration, λ_{write} the wavelength of the laser radiation, λ_{read} the wavelength of the reading (i.e., the wavelength to which the new [changed] refractive index applies [i.e.visible light]), S is the scan speed, and t the line spacing. This detailed equation is based on still unpublished data and modeling (work in progress).

The photochemical model is valid for multiphoton absorption process in a small signal regime without inflicting optical damage or material saturation. In real conditions, the presence of a saturation factor is expected, of which the effect becomes dominant in a large signal regime and prevents the phase change from increasing without bound. As in the previous works [50, 51], in order to apply the photochemical model to the large signal region, a phenomenological saturation factor can effectively limit the maximum induced phase change.

$$\Delta\phi = \frac{\Delta\phi_o}{1 + A/A_{Sat}}$$

where $\Delta\phi_0$ is the small signal induced change, and A represents the parameter driving the saturation (e.g., the induced phase change, the pulse energy, the average power, the irradiated dose).

From the seminal works [50, 51], the saturation phase change as an intrinsic material property is found to decrease with the numerical aperture. It is postulated that the saturated phase change per volume is assumed to be invariant due to a fixed available polymer molecular density or a constant refractive index difference (as result of the ration of molecules and number of displaceable water molecules). As the NA decreases, the interaction volume expands and thus the total saturation phase change within the whole interaction volume increases.

$$A_{\text{Sat,Material}} \cdot NA = \text{constant}$$

In a generalized form (confirmed by the empirical evidence), the wavelength also plays a role in the interaction volume and thus the total saturation phase change.

$$A_{\text{Sat,Material}} \cdot NA \cdot \lambda_{\text{write}} = \text{constant}$$

2.2 Laser induced optical breakdown threshold model

Different materials would have thresholds, and specific laser beam characteristics would lead to a particular threshold for LIOB process. Parameters like pulse duration, tissue properties are considered using previous works [52]. In our simulations, we determine the threshold as being proportional to

$$E_{Th} \propto \sqrt[3]{\tau} \cdot \lambda \cdot \sqrt{m} \cdot M2^2 \cdot NA^{-2}$$

where E_{Th} is the pulse energy threshold for LIOB and $M2$ the beam quality (please note that we consciously used $M2$ for the beam quality, and not the more formal notation M^2. The use of $M2$ as symbol for the parameter aims to avoid confusion with "^{2}" used as exponent (square) in the equations). This detailed equation is a refinement of previous works, based on still unpublished data and modeling (work in progress). The expression was obtained from individual simulations based on the band-gap of water considered as a semiconductor. The values determined for different sets of laser parameters were then fit into unidimensional models, and then combined into a multidimensional expression for the dependence of the LIOB threshold.

2.3 LIRIC at sub-LIOB model

The aim of this work is to present a simple theoretical framework (in the form of a combined model) to determine the optimum laser parameters for maximizing the LIRIC efficiency while staying below the LIOB threshold. Two models are available, one for LIRIC (determining the phase change based on the parameters, and optical power or pulse energy) and one for LIOB (determining the minimum energy necessary to create cavitation bubbles). For both models, higher exponent means more critical/important/decisive parameter. In order to combine them, a qualitative analysis shows that the goal is to "have both models high".

In other words, we search for a parameter space (optical power and pulse energy remain a degree of freedom) in which we can reach a high phase change (large LIRIC) but at the same time enabling a high threshold for optical breakdown, so that no cavitation bubbles will occur in the LIRIC regime (bubbles would only occur for higher energies). The average power at which the LIOB is reached is defined below:

$$P_{Th} = \upsilon \cdot E_{Th}(\tau, \lambda, M2, NA)$$

The rigorous approach is rather simple: the relevant metric is the composite function of both models, i.e., the phase change at a fraction of the threshold energy. i.e., we have to determine the expression for $\Delta\phi[\nu \bullet E_{\text{Th}}(\tau, \lambda, M2, NA)/\text{F}]$, where F is a factor (with $F > 1$) to ensure the irradiation remains significantly below the LIOB threshold.

The semiquantitative optimization is based on the individual relative effect that every parameter has on the induced phase change. By inspecting the exponents, one can determine the relevance of the difference parameters in enhancing the attainable phase change, whereas by evaluating the typical engineering ranges used for the different parameters, an estimate of the quantitative effects can be obtained.

3 Results

3.1 LIRIC at sub-LIOB model

The composite function of both models, i.e., the phase change at a fraction of the threshold energy can be expressed by using the threshold power (P_{Th}) in the photochemical model:

$$\phi = \gamma \frac{{P_{Th}}^{m} \cdot NA^{2(m-2)} \cdot m^{m-2}}{\upsilon^{m-1} \cdot \tau^{m-1} \cdot {\lambda_{write}}^{2m-3} \cdot \lambda_{read} \cdot S \cdot t}$$

$$\Delta\phi = \gamma \frac{\left[\frac{\upsilon \cdot E_{Th}(\tau, \lambda, M2, NA)}{F}\right]^{m} \cdot NA^{2(m-2)} \cdot m^{m-2}}{\upsilon^{m-1} \cdot \tau^{m-1} \cdot {\lambda_{write}}^{2m-3} \cdot \lambda_{read} \cdot S \cdot t}$$

Now substituting the expression for E_{Th} into the photochemical model:

$$\Delta\phi \propto \gamma \frac{[\frac{\upsilon \cdot \sqrt[3]{\tau} \cdot \lambda \cdot \sqrt{m} \cdot M2^2 \cdot NA^{-2}}{F}]^{m} \cdot NA^{2(m-2)} \cdot m^{m-2}}{\upsilon^{m-1} \cdot \tau^{m-1} \cdot {\lambda_{write}}^{2m-3} \cdot \lambda_{read} \cdot S \cdot t}$$

which reduces to:

$$\Delta\phi \propto \gamma \frac{\upsilon \cdot \tau^{-\frac{2m}{3}+1} \cdot {\lambda_{write}}^{3-m} \cdot m^{\frac{3m}{2}-2} \cdot M2^{2m}}{NA^4 \cdot \lambda_{read} \cdot S \cdot t \cdot F^m}$$

of those, v (repetition rate), S (scan speed), and t (line spacing) do not seem to affect the LIOB threshold (E_{Th}) (at least in this model, which does not incorporate any formal damage accumulation effect built-in); whereas m (the order of the multiphoton absorption) affects the LIOB threshold (at least through the associated different wavelength, λ), and $M2$ is not present in the LIRIC model (although probably would behave inversely to NA). Thus, for our purpose, we may simplify the expression to

$$\Delta\phi \propto \gamma \frac{\tau^{-\frac{2m}{3}+1} \cdot {\lambda_{write}}^{3-m} \cdot m^{\frac{3m}{2}-2} \cdot M2^4}{NA^4 \cdot F^m}$$

A higher exponent means more critical/important/decisive parameter. The relevant range for the multiphoton absorption is from $m = 2$ to $m = 6$. This comes from the laser tissue interactions for most polymers (hydrogels, PMMA, or corneal tissue) having a photochemical activation energy corresponding to ~200 nm [14, 50, 51], and 2-photon absorption in the range ~400 nm [51]. This represents $m = 5$ or $m = 6$ for near infrared (NIR) fs irradiations slightly above 1000 nm [52].

3.1.1 Qualitative LIRIC at sub-LIOB model results

The most interesting result is that the effect of NA and $M2$ (in a sense the focusability of the beam) does not depend on the multiphoton order, and yet with an exponent of four both represent a very important parameter. Table 1 summarizes the variables dependencies for different orders of multiphoton absorption.

For two-photon absorption, the effect of the wavelength is linear, shorter pulses help increase the attainable phase change with a minor impact (cubic root of the reciprocal pulse duration), and NA and $M2$ remain the most relevant parameters. For three-photon absorption, the effect of the wavelength cancels out, the pulse duration inversely affects the attainable phase change, and NA and $M2$ remain the most relevant parameters. For four-photon absorption, the pulse duration affects the attainable phase change with a −1.67 exponent; whereas the effect of the wavelength is inversely linear, and NA and $M2$ remain the most relevant parameters. For five-photon absorption, the pulse duration affects the attainable phase change with a −2.33 exponent; whereas the effect of the wavelength is inversely quadratic, and NA and $M2$ remain the most relevant parameters. For six-photon absorption, the pulse duration affects the attainable phase change in an inversely cubic manner; whereas the effect of the wavelength is inversely cubic, with NA and $M2$ all show an exponent of four.

According to the hydrogels experiences [51], the saturation phase change as an intrinsic material property is found to decrease with the numerical aperture, so that NA (and probably $M2$) remains (by far) the most relevant parameter to increase the LIRIC effect without entering the LIOB regime.

Table 1: Multiphoton effects in the LIRIC at sub-LIOB model.

Multiphoton order	Wavelength range (nm) for the human cornea	Expression
2	~270 to ~470	$\Delta\phi(m=2) \propto \tau^{-1/3} \cdot \lambda_{\mathrm{write}} \cdot NA^{-4} \cdot M2^4/F^2$
3	~470 to ~670	$\Delta\phi(m=3) \propto \tau^{-1} \cdot NA^{-4} \cdot M2^4/F^3$
4	~670 to ~860	$\Delta\phi(m=4) \propto \tau^{-5/3} \cdot \lambda_{\mathrm{write}}{}^{-1} \cdot NA^{-4} \cdot M2^4/F^4$
5	~860 to ~1055	$\Delta\phi(m=5) \propto \tau^{-7/3} \cdot \lambda_{\mathrm{write}}{}^{-2} \cdot NA^{-4} \cdot M2^4/F^5$
6	~1055 to ~1455	$\Delta\phi(m=6) \propto \tau^{-3} \cdot \lambda_{\mathrm{write}}{}^{-3} \cdot NA^{-4} \cdot M2^4/F^6$

3.1.2 Quantitative LIRIC at sub-LIOB model results

For hydrogels, it has been shown that 1035 nm correspond to a four-photon photochemical process (including saturation) [50]. The same behavior has been confirmed by our group in an independent experiment (involving a different laser source and optical setup, but using the same hydrogel material, sourcing, and metrology). The system used for the writing process includes a Spark Lasers Altair laser, which delivers femtosecond laser pulses with a pulse duration of ~132 fs, a central wavelength at 1035 ± 5 nm. This laser enables tuneable repetition rate ranging from 5 to 40 MHz via the usage of a pulse picker. The pulse repetition rate from the oscillator is fixed at 40 MHz, and a pulse picker extracts certain pulses from the fast pulse train with an identical temporal separation, resulting in a different repetition rate as selected after the oscillator. The available repetition rates are $40/N$ MHz, where N is an integer number from 1 to 8. An amplifier is employed after the pulse picker to amplify the average power above 10 W and maximum pulse energies above 125 nJ. The effective *NA* for writing the samples goes up to 0.45 using a microscope objective (Thorlabs Inc. LMH-50X-1064). A sample, soaked in saline solution to maintain hydration, is placed between a microscope glass slide and a cover slip. The sample is then mounted on a 2D linear translation stage setup (Physik Instrumente) which allows *XY* axial scanning with a speed up to 1 m/s in *X* direction (stage V-417.056211E1) and a high resolution of about 100 nm in *Y* (stage L-505.013212). A confocal sensor is used to locate the writing depth which is usually set to be in the middle of the polymer sample.

The samples used were plano hydrogels (Contaflex GM Advance 58, Contamac Inc.). Contaflex samples are formed by "Acofilcon A", a synonym for "2-Butenedioic acid (2Z)-, di-2-propenyl ester, polymer with 2,3-Dihydroxypropyl 2-methyl-2-propenoate, 1-Ethenyl-2-pyrrolidinone, 2-Hydroxyethyl 2-methyl-2-propenoate and Methyl 2-methyl-2-propenoate" [51]. The transmissivities of the samples at 1035 nm are greater than 90% [51].

A series of phase bars were written as finely spaced (thus "strong" overlapping) parallel lines. They were fabricated using a raster scanning method. A composite of phase bars of progressively changing pulse energy was meant as a phase carpet. We used pulse energies from 5 to 100 nJ, *NA* from 0.25 to 0.45 via adjusting the incident beam diameter, repetition rates from 5 to 40 MHz, scan speeds from 100 to 1000 mm/s, and line spacing from 100 to 1000 nm. Each phase bar consists of a total width of 150 μm. The length of each grating is set to be 1.5 mm, for which is ensured that a constant velocity inside the bar can be maintained by compensating for the acceleration and deceleration travel distances of the stage. The optical damage was indicated by the formation of cavitation bubbles, or dark carbon spots at higher pulse energies or material distortion with melting traces and porosities localized along the phase bars.

Figure 1 shows a phase carpet consisting of individual phase bars with increasing pulse energy from bottom to top. On the left, the bright field image is presented while the right trace shows an interferogram with coarse interference lines to visually recognize the induced phase shift. In the top bar written with the highest energy, coalescent cavitation bubbles are visible as a sign of the reached LIOB regime. This bar would have been omitted for further analysis.

The results were very much comparable to the previous findings, but we focus more on the sub-LIOB effects. Overall, we generated and measured more than 350 phase

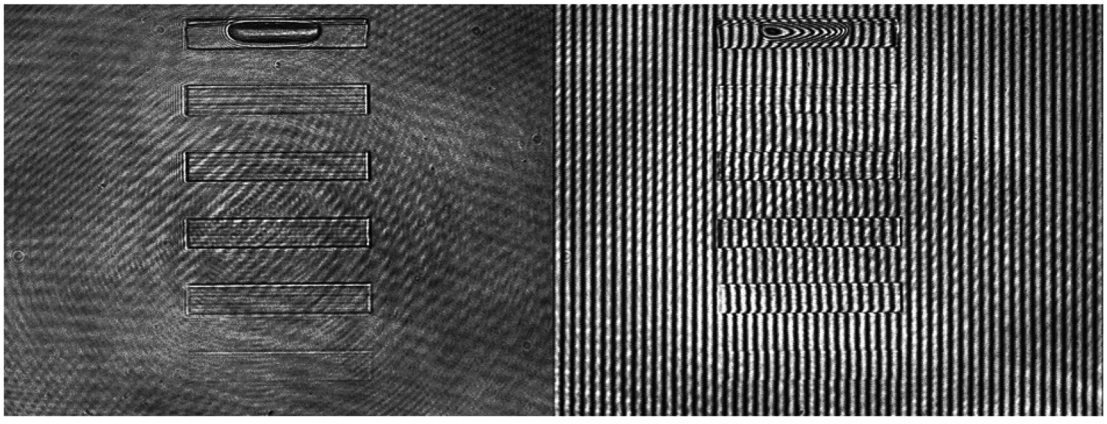

Figure 1: Phase bars with increasing pulse energy from bottom to top. Left: Bright field image. Right: Interferogram with coarse interference lines. In the phase bar with highest pulse energy, coalescent cavitation bubbles are visible as a clear sign of LIOB.

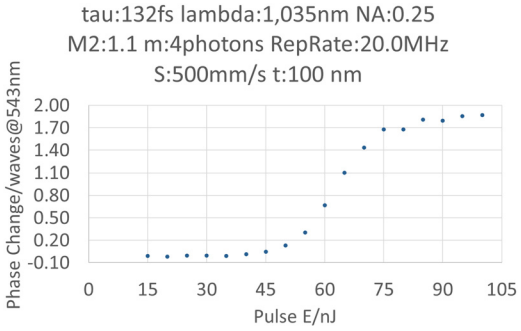

Figure 2: The measured data for the effect of pulse energy on the LIRIC at sub-LIOB attainable effect are presented. Larger pulse energies are associated with higher achieved phase change (scaling to the fourth power in the photochemical process) but limited by a saturation process. This can be seen in the attenuated gain in phase change for high pulse energies.

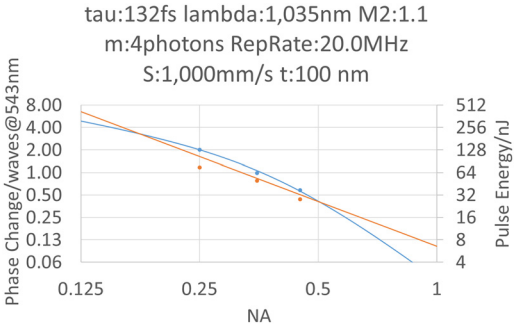

Figure 3: The modeled (solid lines) and measured data (data points) for the effect of *NA* on the LIRIC at sub-LIOB attainable effect are presented. For visualization purposes, a log2 scale has been used for both axes. Both the used energies (determined as E_{Th}/F) (orange series) and achieved phase changes (blue series) match very well the modeled values. Larger *NA* is associated with lower pulse energies, and less achieved phase change. This is actually 3-fold: due to the use of lower pulse energies (scaling to the fourth power in the photochemical process), the smaller focal volume (scaling with the fourth power with the reciprocal of NA), and the lower material saturation (inversely scaling with NA). This can be seen in the attenuated gain in phase change for very low NAs, and the magnified loss of phase change for large NAs.

bars (resulting in 31 phase carpets) in different configurations of pulse energy, *NA*, repetition rate, scan speed, and line spacing.

Figure 2 shows the measured data for the effect of pulse energy on the LIRIC at sub-LIOB attainable effect.

For determining the fraction (factor *F*) below the LIOB threshold we based our analysis on the provisions of the standards on safety for laser products [53, 54]. They request different levels of protective measures for energies exceeding +20, +50, and +100% of the nominally set energy. Applied to our case, it would mean that in order to remain below the LIOB regime, the maximum nominally set energy should not exceed $E_{Th}/1.2$, $E_{Th}/1.5$, or $E_{Th}/2.0$, respectively. For the presentation of results, we select the intermediate factor $F = 1.5$ ($E_{Th}/1.5$).

With these reduced energies (below LIOB threshold) we have determined the induced phase change (including saturation effects) as a function of the individual parameters governing the induced phase change. Figures 3 and 4 show those dependencies for the most relevant parameters considered in the photochemical model.

Figure 3 shows the modeled and measured data for the effect of *NA* on the attainable LIRIC effect at sub-LIOB.

In our experiments, we have neither modified the pulse duration (which would have been possible within a range towards longer pulses, which would further reduce the measurable phase changes) nor the wavelength (fixed in our system and laser source, reachable via harmonic generators though). Recent published data for 405 nm ($m = 2$) and 1035 nm ($m = 4$) wavelengths are available [50, 51]. These works provide the gains (material constants) for the respective wavelengths. These reported gains (material constants) have been used to estimate its value for the intermediate case ($m = 3$) as the geometric mean of the 405 and 1035 nm constants. Further, the phenomenological saturation factor incorporates both *NA* and wavelength dependences, as stated under 2.1.

Figure 4 shows the modeled data for the effect of pulse duration and wavelength on the LIRIC at sub-LIOB attainable effect. A shorter pulse duration is associated with lower pulse energies, but a higher achieved phase change. This is because the effect of the pulse duration in the LIOB threshold only affects with the cubic root of τ, but with the cubic power of the reciprocal of τ in the four-photon photochemical model. This can be seen in the attenuated gain in phase change for very short pulses, and the magnified loss of phase change for long pulse durations. Longer wavelengths are associated with higher pulse energies, but less achieved phase change. The relationship with wavelength is rather complex, involving changes in the material constant (γ, a sort of gain of the process), the photon energy, and the order of the multiphoton absorption. For both effects (pulse duration and wavelength dependence), the number of photons per space and time becomes essential. For higher order processes it becomes increasingly important, that m-photons (the order of the multiphoton absorption) reach the region of interest (where laser-tissue interactions are expected) at the "same" time to be quasi-simultaneously absorbed. This provides a hint that for multiphoton processes, shorter pulses (for the same pulse energy more photons are available per unit of time, increasing the peak power of the pulse) or shorter wavelengths (irradiating

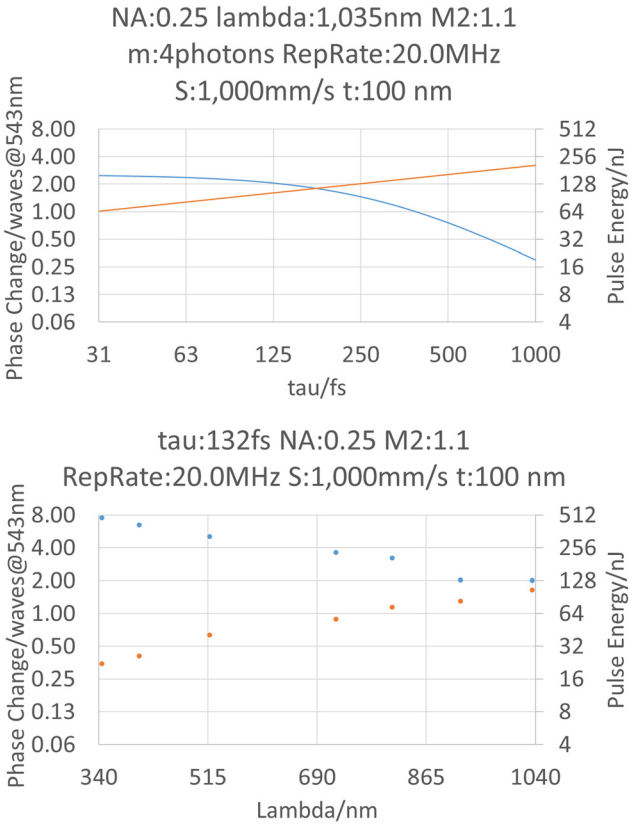

Figure 4: The modeled data for the effect of pulse duration (left panel) and wavelength (right panel) on the LIRIC at sub-LIOB attainable effect are presented. For visualization purposes, a log2 scale has been used for the phase change and the pulse energy. The used energies (determined as E_{Th}/F) (orange series) and achieved phase changes (blue series) are depicted for individual wavelengths. A shorter pulse duration is associated with lower pulse energies (in orange in the left panel), but a higher achieved phase change (in blue in the left panel). This is because the effect of the pulse duration in the LIOB threshold only affects with the cubic root of τ, but with the cubic power of the reciprocal of τ in the 4-photon photochemical model. This can be seen in the attenuated gain in phase change for very short pulses, and the magnified loss of phase change for long pulse durations. Longer wavelengths are associated with higher pulse energies (in orange in the right panel), but less achieved phase change (in blue in the right panel). The relationship with wavelength is rather complex, involving changes in the material constant (γ, a sort of gain of the process), the photon energy, and the order of the multiphoton absorption.

photons of higher energy, reducing the number of photons required to reach the region of interest at the "same" time) become very important parameters for enhancing the efficiency of the processes.

4 Discussion

We present here a simple method to determine the optimum laser parameters for maximizing the LIRIC efficiency for pulse energies below the LIOB threshold for different materials (in particular, polymers such as hydrogels or the human cornea) for which the multiphoton order of the photochemical model is known or can be estimated. The model combines two independent previous models in a simple manner [51, 52]. The work provides qualitative and quantitative estimates for the parameters leading to a maximum LIRIC effect below the threshold of LIOB.

The photochemical model is valid for multiphoton absorption process in a small signal regime without creating optical damage or material saturation. For that reason, approaches avoiding optical damage actually legitimate the use of that photochemical model.

In the formulation of the photochemical model, a correction for the readout laser wavelength has been taken into account. In the general case, the writing wavelength is different than the readout wavelength. However, for a fixed readout wavelength (likely close to the center of the visible spectrum for the human eye), this effect may change the values of the measured phase change, but not its dependence on other parameters. In a sense, this correcting factor can be incorporated into the gain (scaling) factor of the LIRIC process.

We used the LIOB model as the main descriptor for the optical damage, yet there may be other competing mechanisms (with onset at different power regimes, e.g., thermal mechanisms) which may produce a different type of optical damage for some of the tested conditions [55].

The used LIOB threshold model is by definition independent of the laser repetition rate (i.e., LIOB is a per pulse process). For some hydrogels (but not for the one used in this work) [51], optical damages have been reported to occur at lower energies for faster laser repetition rates but this has not been elucidated for the human cornea.

The LIOB threshold model determined the single pulse damage, thus it is not dependent on *S* scan speed or *t* line spacing. We acknowledge as a limitation, that this "simple" model does not include the effects of multipulse accumulation on the pulse energy damage level. This complex process has been experimentally explored for pulse energies well above the LIOB threshold in previous works [56, 57].

We did not present results for different *S* (scan speed), and *t* (line spacing) since they do not seem to affect the LIOB threshold, and the effect of *M2* was made analogous to *NA* (but it has not been further investigated; potentially a similar effect would be found for the Strehl Ratio of the system since it also affects the focusability of the beam).

The most interesting result is that the effect of *NA* and *M2* (in a sense the focusability of the beam) does not depend on the multiphoton order, and yet with an exponent of 4 both represent a very important parameter. For both effects (*NA* and *M2*), the number of photons per space and time becomes essential. For higher order processes it becomes increasingly important that m-photons (the order of the multiphoton absorption) reach the region of interest (where laser-tissue interactions are expected) at the "same" time to be quasi-simultaneously absorbed.

The presented results were obtained using a four-photon model (consistent with the findings published for hydrogels), but for the human cornea most probably a five-photon model would be required (corresponding to lower phase changes). For four-photon absorption (wavelength range ~670 to ~860 nm for the cornea), the pulse duration affects the attainable phase change with a –1.67 exponent; whereas the effect of the wavelength is inversely linear, and *NA* and *M2* remain the most relevant parameters. On the contrary, for five-photon absorption (wavelength range ~860 to ~1055 nm for the cornea), the pulse duration affects the attainable phase change with a –2.33 exponent; whereas the effect of the wavelength is inversely quadratic, and *NA* and *M2* remain the most relevant parameters.

Essentially, the approach is to search for the parameters leading to a higher LIOB threshold (in order to benefit from the multiphoton scaling of phase change with pulse energy), which are not detrimental to the LIRIC process. In real conditions, the presence of a saturation factor is expected, of which the effect becomes dominant in a large signal regime and prevents the phase change from increasing without bound. Based on our empiric data at 1035 nm, the phenomenological saturation factor for the used hydrogel was found to be 2.5 waves at *NA* of 0.25, 1.7 waves at *NA* of 0.38, and 1.4 waves at *NA* of 0.45.

The measured data for the effect of pulse energy on the LIRIC at sub-LIOB attainable effect (Figure 2) shows that larger pulse energies are associated with higher achieved phase change (scaling to the fourth power in the photochemical process) but limited by a saturation process or other competing effects induced at higher energies, which are not explicitly included in this model.

According to the hydrogels experiences [51] and the presented findings, the saturation phase change as an intrinsic material property is found to decrease with the numerical aperture increases. As shown in the derivation of the photochemical model, this is due to the larger volume treated at lower numerical apertures. A larger affected volume subsequently induces a larger optical phase shift due to the definition of optical phase (the product of refractive index and physical thickness). It remains unclear though whether this effect can be extrapolated to corneal tissue.

For determining the fraction (factor *F*) below the LIOB threshold we based on the provisions of the international standards on safety for laser products [53, 54]. For the presentation of results, we select the intermediate factor $F = 1.5$. The numeric results would have been different for other factors (higher for $F = 1.2$; lower for $F = 2.0$), but the overall behavior would have been retained. Since the phase change scales with the fourth power of the pulse energy, working as close as possible (but below) the threshold may be more beneficial. Although, due to the presence of the saturation, the use of a factor $F = 1.5$ seems sufficient (and reduces the imparted dose to the tissue).

Using a moderate *NA* between 0.2 and 0.3 seems to be more adequate to maximize LIRIC efficiency (at the cost of affecting a thicker layer of tissue). A reduction from 0.45 to 0.25 *NA* produced a 3.3× fold increase in the attained phase change (for a 3.0× increase in pulse energy).

Using pulse durations shorter than 175 fs seems to be more adequate to maximize LIRIC efficiency (at the cost of reducing pulse energy, thus requiring more accurate controls of the pulse energy). A reduction from 175 to 50 fs predicts a 1.3× increase in the attained phase change (for a 0.66× decrease in pulse energy). Using shorter wavelengths seems to be more adequate to maximize LIRIC efficiency due to a lower and thus more efficient absorption order (at the cost of reducing pulse energy, thus requiring more accurate

controls of the pulse energy). A reduction from 1035 to 405 nm predicts a 2.4× increase in the attained phase change (for a 0.25× decrease in pulse energy). However, eye safety imposes lower maximum permissible exposures at shorter wavelengths [58].

5 Conclusions

In summary, we presented a method to determine the adequate ranges for the most relevant parameters for maximizing the LIRIC efficiency for pulse energies below the LIOB threshold for different materials (in particular, polymers such as hydrogels or the human cornea). Essentially, the approach is to search for the parameters leading to a higher LIOB threshold (in order to benefit from the multiphoton scaling of phase change with pulse energy), which are not detrimental to the LIRIC process. The model suggests that the use of a moderate *NA* ~0.24, combined with pulse durations shorter than 100 fs seems to be more adequate to maximize LIRIC efficiency. Using shorter wavelengths still in the NIR region (~800 nm) may further enhance LIRIC efficiency (by reducing the multiphoton order by one unit).

Author contributions: All the authors have accepted responsibility for the entire content of this submitted manuscript and approved submission.
Research funding: None declared.
Conflict of interest statement: SAM, LK, PN and SV are employees of SCHWIND eye-tech-solutions. SS is an employee of Light Conversion. WHK is Chief Science Officer at Clerio Vision, with no management or fiduciary responsibilities. LZ is an employee of Clerio Vision, Inc.

References

[1] S. L. Trokel, R. Srinivasan, and B. Braren, "Excimer laser surgery of the cornea," *Am. J. Ophthalmol.*, vol. 96, pp. 710–715, 1983.
[2] A. Antón, M. T. Andrada, A. Mayo, J. Portela, and J. Merayo, "Epidemiology of refractive errors in an adult european population: the Segovia study," *J. Ophthalmic. Epidemiol.*, vol. 16, pp. 231–237, 2009.
[3] S. Gomez, J. Herreras, J. M. Merayo-Lloves, M. García, P. Argueso, and J. Cuevas, "Effect of hyaluronic acid on corneal haze in a photorefractive keratectomy experimental model," *J. Refract. Surg.*, vol. 17, pp. 549–554, 2001.
[4] R. M. Torres, J. M. Merayo-Lloves, J. T. Blanco-Mezquita, et al., "Experimental model of laser assisted in situ keratomileusis in hens," *J. Refract. Surg.*, vol. 21, pp. 392–398, 2005.
[5] S. Kling, L. Remon, A. Pérez-Escudero, J. Merayo-Lloves, S. Susana Marcos, "Corneal biomechanical changes after collagen cross-linking from porcine eye inflation experiments," *Investig. Ophthalmol. Vis. Sci.*, vol. 51, no. 8, pp. 3961–3968, 2010.
[6] J. L. Alió, M. Helmy Shabayek, R. Montes-Mico, et al., "Intracorneal hydrogel lenses and corneal aberrations," *J. Refract. Surg.*, vol. 21, pp. 247–252, 2005.
[7] C. Martínez García, J. M. Merayo-Lloves, T. Blanco Mezquita, and S. Mar Sardaña, "Wound healing following refractive surgery in hens," *Exp. Eye Res.*, vol. 83, no. 4, pp. 728–735, 2006.
[8] J. Del Val, S. Barrero, B. Yañez, et al., "Experimental measurement of corneal haze after excimer laser keratectomy," *Appl. Opt.*, vol. 40, pp. 1727–1731, 2001.
[9] J. M. Merayo-Lloves, B. P. Yañez, A. Mayo, R. Martín, and J. C. Pastor, "Experimental model of corneal haze in chickens," *J. Refract. Surg.*, vol. 17, pp. 696–699, 2001.
[10] Gould G. Laser. US patent: US19590804539 19590406; 1959.
[11] A. L. Schawlow, and C. H. Townes, "Infrared and optical masers," *Phys. Rev.*, vol. 112, pp. 1940–1949, 1958.
[12] C. A. Swinger, "Refractive surgery for the correction of myopia," *Trans. Ophthalmol. Soc. U. K.*, vol. 101, pp. 434–439, 1981.
[13] C. R. Munnerlyn, S. J. Koons, and J. Marshall, "Photorefractive keratectomy: a technique for laser refractive surgery," *J. Cataract Refract. Surg.*, vol. 14, pp. 46–52, 1988.
[14] R. R. Krueger, and S. L. Trokel, "Quantitation of corneal ablation by ultraviolet laser light," *Arch. Ophthalmol.*, vol. 103, pp. 1741–1742, 1985.
[15] G. H. Pettit, M. N. Ediger, and R. P. Weiblinger, "Excimer laser corneal ablation: absence of a significant "incubation" effect," *Laser Surg. Med.*, vol. 11, pp. 411–418, 1991.
[16] T. Seiler, U. Genth, A. Holschbach, and M. Derse, "Aspheric photorefractive keratectomy with excimer laser," *Refract. Corneal Surg.*, vol. 9, pp. 166–172, 1993.
[17] L. Mastropasqua, L. Toto, E. Zuppardi, et al., "Photorefractive keratectomy with aspheric profile of ablation versus conventional photorefractive keratectomy for myopia correction: six-month controlled clinical trial," *J. Cataract Refract. Surg.*, vol. 32, pp. 109–116, 2006.
[18] C. Kirwan, and M. O'Keefe, "Comparative study of higher-order aberrations after conventional laser in situ keratomileusis and laser epithelial keratomileusis for myopia using the technolas 217z laser platform," *Am. J. Ophthalmol.*, vol. 147, pp. 77–83, 2009.
[19] R. R. Krueger, T. Juhasz, A. Gualano, and V. Marchi, "The picosecond laser for nonmechanical laser in situ keratomileusis," *J. Refract. Surg.*, vol. 14, no. 4, pp. 467–469, 1998.
[20] D. S. Durrie, S. G. Slade, and J. Marshall, "Wavefront-guided excimer laser ablation using photorefractive keratectomy and sub-Bowman's keratomileusis: a contralateral eye study," *J. Refract. Surg.*, vol. 24, no. 1, pp. S77–S84, 2008.
[21] W. Sekundo, K. Kunert, C. Russmann, et al., "First efficacy and safety study of femtosecond lenticule extraction for the correction of myopia: six-month results," *J. Cataract Refract. Surg.*, vol. 34, no. 9, pp. 1513–1520, 2008.
[22] W. Sekundo, K. S. Kunert, and M. Blum, "Small incision corneal refractive surgery using the small incision lenticule extraction (SMILE) procedure for the correction of myopia and myopic astigmatism: results of a 6 month prospective study," *Br. J. Ophthalmol.*, vol. 95, no. 3, pp. 335–339, 2011.
[23] I. Ratkay-Traub, I. E. Ferincz, T. Juhasz, R. M. Kurtz, and R. R. Krueger, "First clinical results with the femtosecond

neodymium-glass laser in refractive surgery," *J. Refract. Surg.*, vol. 19, no. 2, pp. 94–103, 2003.

[24] A. Heisterkamp, T. Mamom, O. Kermani, et al., "Intrastromal refractive surgery with ultrashort laser pulses: in vivo study on the rabbit eye," *Graefes Arch. Clin. Exp. Ophthalmol.*, vol. 241, no. 6, pp. 511–517, 2003.

[25] J. H. Talamo, J. Meltzer, and J. Gardner, "Reproducibility of flap thickness with IntraLase FS and moria LSK-1 and M2 microkeratomes," *J. Refract. Surg.*, vol. 22, no. 6, pp. 556–561, 2006.

[26] Y. Zhou, L. Tian, N. Wang, and P. J. Dougherty, "Anterior segment optical coherence tomography measurement of LASIK flaps: femtosecond laser vs microkeratome," *J. Refract. Surg.*, vol. 27, no. 6, pp. 408–416, 2011.

[27] J. Javaloy, M. T. Vidal, A. M. Abdelrahman, A. Artola, and J. L. Alvió, "Confocal microscopy comparison of intralase femtosecond laser and Moria M2 microkeratome in LASIK," *J. Refract. Surg.*, vol. 23, no. 2, pp. 178–187, 2007.

[28] I. Guber, L. Moetteli, L. Magnin, and F. Majo, "Moving from a mechanical microkeratome to a femtosecond laser for LASIK to correct astigmatic patients: clinical outcomes of a retrospective, consecutive, comparative study," *Klin. Monbl. Augenheilkd.*, vol. 230, no. 4, pp. 337–341, 2013.

[29] G. M. Kezirian, and K. G. Stonecipher, "Comparison of the IntraLase femtosecond laser and mechanical keratomes for laser in situ keratomileusis," *J. Cataract Refract. Surg.*, vol. 30, no. 4, pp. 804–811, 2004.

[30] K. Stonecipher, T. S. Ignacio, and M. Stonecipher, "Advances in refractive surgery: microkeratome and femtosecond laser flap creation in relation to safety, efficacy, predictability, and biomechanical stability," *Curr. Opin. Ophthalmol.*, vol. 17, no. 4, pp. 368–372, 2006.

[31] M. V. Netto, R. R. Mohan, F. W. Medeiros, et al., "Femtosecond laser and microkeratome corneal flaps: comparison of stromal wound healing and inflammation," *J. Refract. Surg.*, vol. 23, no. 7, pp. 667–676, 2007.

[32] R. Gil-Cazorla, M. A. Teus, L. de Benito-Llopis, and I. Fuentes, "Incidence of diffuse lamellar keratitis after laser in situ keratomileusis associated with the IntraLase 15 kHz femtosecond laser and Moria M2 microkeratome," *J. Cataract Refract. Surg.*, vol. 34, no. 1, pp. 28–31, 2008.

[33] Y. Wang, J. Li, Y. Liu, and L. Xie, "Intraocular stray light after thin-flap LASIK with a femtosecond laser versus a mechanical microkeratome," *J. Refract. Surg.*, vol. 29, no. 8, pp. 534–539, 2013.

[34] M. A. Sarayba, T. S. Ignacio, P. S. Binder, and D. B. Tran, "Comparative study of stromal bed quality by using mechanical, IntraLase femtosecond laser 15- and 30-kHz microkeratomes," *Cornea*, vol. 26, no. 4, pp. 446–451, 2007.

[35] H. Ahn, J. K. Kim, C. K. Kim, et al., "Comparison of laser in situ keratomileusis flaps created by 3 femtosecond lasers and a microkeratome," *J. Cataract Refract. Surg.*, vol. 37, no. 2, pp. 349–357, 2011.

[36] J. M. Vetter, M. Faust, A. Gericke, N. Pfeiffer, W. E. Weingärtner, and W. Sekundo, "Intraocular pressure measurements during flap preparation using 2 femtosecond lasers and 1 microkeratome in human donor eyes," *J. Cataract Refract. Surg.*, vol. 38, no. 11, pp. 2011–2018, 2012.

[37] D. Giguère, G. Olivié, F. Vidal, et al., "Laser ablation threshold dependence on pulse duration for fused silica and corneal tissues: experiments and modeling," *J. Opt. Soc. Am. Opt Image Sci. Vis.*, vol. 24, no. 6, pp. 1562–1568, 2007.

[38] G. D. Kymionis, V. P. Kankariya, A. D. Plaka, and D. Z. Reinstein, "Femtosecond laser technology in corneal refractive surgery: a review," *J. Refract. Surg.*, vol. 28, no. 12, pp. 912–920, 2012.

[39] R. Shah, S. Shah, and S. Sengupta, "Results of small incision lenticule extraction: all-in-one femtosecond laser refractive surgery," *J. Cataract Refract. Surg.*, vol. 37, pp. 127–137, 2011.

[40] M. Ang, D. Tan, and J. S. Mehta, "Small incision lenticule extraction (SMILE) versus laser in-situ keratomileusis (LASIK): study protocol for a randomized, non-inferiority trial," *Trials*, vol. 13, p. 75, 2012.

[41] Juhasz T. Method for corneal laser surgery. Applicant: ESCALON MEDICAL CORP. Filed in 1996; Granted in 2000; Published in 1998. Available at: http://worldwide.espacenet.com/publicationDetails/biblio?DB=worldwide.espacenet.com&II=3&ND=3&adjacent=true&locale=en_EP&FT=D&date=20000829&CC=US&NR=6110166A&KC=A.

[42] M. Blum, K. Täubig, C. Gruhn, W. Sekundo, and K. S. Kunert, "Five-year results of small incision lenticule extraction (ReLEx SMILE)," *Br. J. Ophthalmol.*, vol. 100, no. 9, pp. 1192–1195, 2016.

[43] K. R. Pradhan, and S. Arba Mosquera, "Three-month outcomes of myopic astigmatism correction with small incision guided human-cornea treatment," *J. Refract. Surg.*, vol. 37, no. 5, pp. 304–311, 2021.

[44] L. Izquierdo, Jr., D. Sossa, O. Ben-Shaul, and M. A. Henriquez, "Corneal lenticule extraction assisted by a low-energy femtosecond laser," *J. Cataract Refract. Surg.*, vol. 46, no. 9, pp. 1217–1221, 2020.

[45] M. He, W. Huang, and X. Zhong, "Central corneal sensitivity after small incision lenticule extraction versus femtosecond laser-assisted LASIK for myopia: a meta-analysis of comparative studies," *BMC Ophthalmol.*, vol. 15, p. 141, 2015.

[46] R. Dou, Y. Wang, L. Xu, D. Wu, W. Wu, and X. Li, "Comparison of corneal biomechanical characteristics after surface ablation refractive surgery and novel lamellar refractive surgery," *Cornea*, vol. 34, pp. 1441–1446, 2015.

[47] M. Elling, I. Kersten-Gomez, and H. B. Dick, "Photorefractive intrastromal corneal crosslinking for treatment of myopic refractive error: findings from 12-month prospective study using an epithelium-off protocol," *J. Cataract Refract. Surg.*, vol. 44, no. 4, pp. 487–495, 2018.

[48] D. E. Savage, D. R. Brooks, M. DeMagistris, et al., "First demonstration of ocular refractive change using blue-IRIS in live cats," *Invest. Ophthalmol. Vis. Sci.*, vol. 55, no. 7, pp. 4603–4612, 2014.

[49] L. Ding, R. Blackwell, J. F. Kunzler, and W. H. Knox, "Large refractive index change in silicone-based and non-silicone-based hydrogel polymers induced by femtosecond laser micro-machining," *Opt Express*, vol. 14, no. 24, pp. 11901–11909, 2006.

[50] R. Huang, and W. H. Knox, "Quantitative photochemical scaling model for femtosecond laser micromachining of ophthalmic hydrogel polymers: effect of repetition rate and laser power in the four photon absorption limit," *Opt. Mater. Express*, vol. 9, pp. 1049–1061, 2019.

[51] R. Huang, and W. H. Knox, "Femtosecond micro-machining of hydrogels: parametric study and photochemical model including material saturation," *Opt. Mater. Express*, vol. 9, pp. 3818–3834, 2019.

[52] J. Noack, and A. Vogel, "Laser-induced plasma formation in water at nanosecond to femtosecond time scales: calculation of thresholds, absorption coefficients, and energy density," *IEEE J. Quant. Electron.*, vol. 35, no. 8, pp. 1156–1167, 1999.
[53] IEC 60825, "Series on safety of laser products," 2021.
[54] IEC 60601-2-22, "Medical electrical equipment - part 2–22: particular requirements for basic safety and essential performance of surgical, cosmetic, therapeutic and diagnostic laser equipment," 2019.
[55] D. Sola, J. R. Aldana, and P. Artal, "The role of thermal accumulation on the fabrication of diffraction gratings in ophthalmic PHEMA by ultrashort laser direct writing," *Polymers*, vol. 12, no. 12, p. 2965, 2020.
[56] N. Tinne, E. Lübking, H. Lubatschowski, A. Krüger, and T. Ripken, "The influence of a spatial and temporal pulse-overlap on the laser-tissue-interaction of modern ophthalmic laser systems," *Biomed. Tech. (Berl)*, vol. 57, no. Suppl. 1, 2012, https://doi.org/10.1515/bmt-2012-4115.
[57] E. Saerchen, S. Liedtke-Gruener, M. Kopp, A. Heisterkamp, H. Lubatschowski, and T. Ripken, "Femtosecond laser induced step-like structures inside transparent hydrogel due to laser induced threshold reduction," *PLoS One*, vol. 14, no. 9, p. e0222293, 2019.
[58] International Commission on Non-Ionizing Radiation Protection, "Revision of guidelines on limits of exposure to laser radiation of wavelengths between 400 nm and 1.4 micron," *Health Phys.*, vol. 79, no. 4, pp. 431–440, 2000.